

Robustness of critical U(1) spin liquids and emergent symmetries in tensor networks

Henrik Dreyer,^{1,2} Laurens Vanderstraeten,³ Ji-Yao Chen^{①,1,2}, Ruben Verresen,⁴ and Norbert Schuch^{①,1,2,5,6}

¹*Max-Planck-Institute of Quantum Optics, Hans-Kopfermann-Straße 1, 85748 Garching, Germany*

²*Munich Center for Quantum Science and Technology, Schellingstraße 4, 80799 München, Germany*

³*Department of Physics and Astronomy, Ghent University, Krijgslaan 281, S9, 9000 Gent, Belgium*

⁴*Department of Physics, Harvard University, Cambridge, Massachusetts 02138, USA*

⁵*University of Vienna, Faculty of Mathematics, Oskar-Morgenstern-Platz 1, 1090 Wien, Austria*

⁶*University of Vienna, Faculty of Physics, Boltzmannngasse 5, 1090 Wien, Austria*



(Received 3 January 2024; accepted 6 May 2024; published 21 May 2024)

We study the response of critical resonating valence bond (RVB) spin liquids to doping with longer-range singlets, and more generally of U(1)-symmetric tensor networks to nonsymmetric perturbations. Using a field theory description, we find that in the RVB, doping constitutes a relevant perturbation that immediately opens up a gap, contrary to previous observations. Our analysis predicts a very large correlation length even at significant doping, which we verify using high-accuracy numerical simulations. This emphasizes the need for careful analysis, but it also justifies the use of such states as a variational ansatz for critical systems. Finally, we give an example of a projected entangled pair state where nonsymmetric perturbations do not open up a gap and the U(1) symmetry reemerges.

DOI: [10.1103/PhysRevB.109.195161](https://doi.org/10.1103/PhysRevB.109.195161)

Projected entangled pair states (PEPS) form a powerful analytical and numerical framework for describing strongly correlated quantum systems, such as spin liquids or systems with topological order [1–7]. Their power stems from the local description where a tensor correlates physical and entanglement degrees of freedom. A key strength of PEPS is the encoding of physical symmetries in symmetries of the tensor, which allows us to locally impose, probe, and control desired properties, and is central to applications ranging from the classification of phases all the way to efficient algorithms [7–16].

However, it is not only physical symmetries that are reflected in the tensor: PEPS can exhibit symmetries acting purely on the entanglement degrees of freedom, which are deeply connected to both topological order and critical behavior, and closely tied to a Gauss law of the underlying field theory. In particular, topological order in two dimensions (2D) is accompanied by entanglement symmetries that act as representations of a discrete group (or some more general algebraic structure), such as \mathbb{Z}_2 for the toric code model [17–19]. Another such connection is between continuous symmetries, in particular U(1), and criticality. A key example in which this occurs is the dimer model and the spin- $\frac{1}{2}$ resonating valence bond (RVB) state on bipartite lattices, which has been studied in depth since Anderson proposed it as an ansatz

wave function for the parent state of the high- T_c cuprate superconductors [20,21].

But how closely are these symmetries linked to the physics observed—are they strictly necessary, or do they just happen to appear in the specific PEPS representation used? This is of central importance for the construction of variational ansätze, since it determines whether we need to stabilize said symmetry to be able to capture certain physics, such as topological order or criticality. In the case of topological order, breaking the discrete entanglement symmetry induces doping with quasiparticles, which in 2D immediately destroys topological order beyond a certain length scale, just as finite temperature [22,23] (but not in 3D [24,25]), and thus hardwiring those symmetries is essential to obtain a wave function with true topological order.

For continuous entanglement symmetries such as U(1) in critical systems, the situation is less clear. For instance, in the RVB and dimer model, doping with longer-range (LR) singlets will generally break the U(1) symmetry. However, for PEPS models that realize such doping, evidence for an extended critical regime up to significant doping has been observed when studying them as variational ansätze for frustrated Heisenberg models, such as the $J_1 - J_2$ model on the square lattice [26,27]. This raises several questions: Can one refrain from stabilizing the U(1) symmetry when aiming for a critical wave function? Could stability of the critical phase point to an *emergent* U(1) symmetry, something not yet observed in PEPS, and different from what is seen for 2D PEPS with discrete symmetries and topological order? Finally, can we understand this in terms of the underlying field theory, just as the breakdown of topological order under perturbation can be explained from quasiparticle doping?

Published by the American Physical Society under the terms of the [Creative Commons Attribution 4.0 International](https://creativecommons.org/licenses/by/4.0/) license. Further distribution of this work must maintain attribution to the author(s) and the published article's title, journal citation, and DOI. Open access publication funded by Max Planck Society.

In this paper, we study critical spin liquids with a PEPS representation with a $U(1)$ entanglement symmetry, and we investigate their robustness under perturbations away from the $U(1)$ point, with the RVB state with LR singlets as our guiding example. To this end, we employ an effective field theory description, treating the transfer matrix as a Luttinger liquid with parameter K . This allows us to analyze the perturbations away from the $U(1)$ point as perturbations in the field theory. Applying this to the RVB and dimer PEPS doped with LR singlets reveals that this is a relevant perturbation and thus should open up a gap immediately. However, a scaling analysis reveals that for the RVB state, the gap opens up extremely slowly, which explains why this gap has not been observed in previous simulations. We support our analysis by high-precision numerics, from which we can reliably extract correlation lengths on the order of 10^4 sites, far beyond what had been observed before. The results match well with the scaling analysis as well as a more quantitative prediction based on the sine-Gordon model. Our findings are not limited to the RVB model, but they apply generally to PEPS with a $U(1)$ entanglement symmetry and $K > \frac{1}{2}$.

We conclude by discussing ways to obtain models where such perturbations do not open up a gap and thus give rise to an emergent $U(1)$ symmetry. We provide an example of a PEPS wave function where field theory predicts such a robustness, and we give numerical evidence that under $U(1)$ -breaking perturbations, the $U(1)$ symmetry reemerges.

Let us start by introducing the RVB and dimer model [20,21]. Throughout the paper, it will serve as our guiding example, even though our key findings apply in generality. The dimer model on the square lattice is the equal weight superposition $|\Psi\rangle = \sum |D\rangle$ of all coverings $|D\rangle$ of the lattice with nearest-neighbor dimers [Fig. 1(a)]; the RVB model is obtained by replacing the dimers by spin- $\frac{1}{2}$ singlets $|\sigma(D)\rangle$, oriented from the A to B sublattice. The RVB and dimer model have natural PEPS representations, Fig. 1(b) [2,28]: The tensor $P_{i_{\text{hard}}}^i$ is constructed such that the *physical index* $i = 0, 1$ is identified with any one of the four *virtual indices* $l, r, u, d = 0, 1, 2$, while the other three take the value 2, such that the tensor has the point-group symmetry. By arranging these tensors on a square grid and contracting adjacent virtual indices with a singlet in between, we obtain the RVB state. Similarly, we can construct a PEPS for the dimer model by adding another physical index at each site, which duplicates the information along which direction the singlet is placed [28]. We label these two settings by $|\sigma_g(D)\rangle$, $|\Psi_g\rangle = \sum |\sigma_g(D)\rangle$, where $g = 0$ corresponds to the RVB and $g = 1$ to the dimer model.

The RVB and dimer model naturally possess a $U(1)$ Gauss law: given any region with an identical number of A and B sublattice sites, consider all singlets that cross the boundary of the region, and count how many of them cover an A sublattice vertex inside the region, versus how many cover a B sublattice vertex. The difference of these two numbers is always zero, since each singlet that sits fully inside the region covers one A and one B vertex each, leaving an equal number of A and B vertices to be paired up with outside vertices. In the PEPS representation, Gauss' law can be seen as follows, illustrated in Fig. 1(a): Each tensor has exactly three virtual indices in the state $|2\rangle$ (i.e., no singlet), while the fourth is in the subspace spanned by $\{|0\rangle, |1\rangle\}$ (singlet); if we assign a

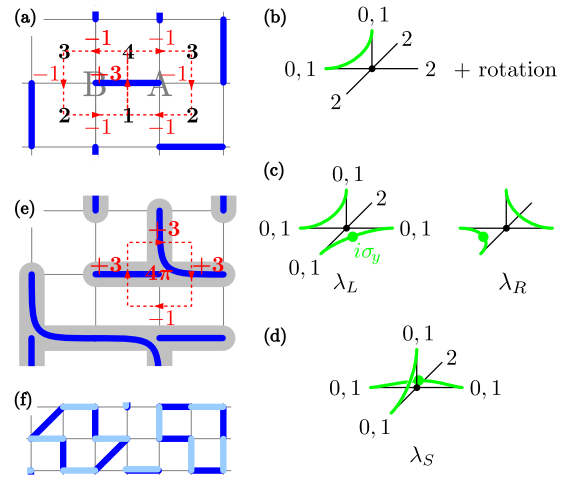


FIG. 1. (a) RVB and dimer model. Numbers in the plaquettes are the height potential $h(\vec{x})$ obtained from the $U(1)$ Gauss law (red). (b) PEPS tensor for the RVB state. The green line is the identity on the $\{|0\rangle, |1\rangle\}$ space, and all rotations are summed. (c) Tensors with “teleportation bonds,” which give rise to longer-range singlets; the two tensors are related by reflection. (d) For $-\lambda_L = \lambda_R$, the sum of the two tensors in (c) is equivalent to the tensor shown with only straight teleportation bonds, explaining the observed absence of diagonal AA-singlets [26]. (e) Model with longer-range singlets (c), and the “dimer-solidomer” model (gray). The teleportation tensors carry a flux $2\pi m = 4\pi$. (f) Overlap of two singlet configurations in the RVB, forming loops. Loops must contain an even number of same-sublattice singlets. Since configurations with more loops are favored, in expectation values same-sublattice singlets tend to come in (ket-ket or ket-bra) pairs.

weight -1 to each $|2\rangle$ state and a weight $+3$ to states in the $\{|0\rangle, |1\rangle\}$ subspace, this adds up to zero and thus gives rise to a $U(1)$ entanglement symmetry of the tensor. This allows us to derive a potential, the *height representation* [29–31], where we assign to every plaquette a height $h(\vec{x})$ that changes by $+3$ when crossing a dimer clockwise (counterclockwise) around an A (B) sublattice vertex, and by -1 otherwise. While for expectation values $\langle \Psi_g | \Psi_g \rangle = \sum_{D, D'} \langle \sigma_g(D) | \sigma_g(D') \rangle$, separate height fields h, h' are associated with ket and bra, it has been demonstrated in Ref. [32] that they are locked together in the long-wavelength limit and can thus be replaced by a single field. Intuitively, this can be understood as follows (we refer the interested reader to Ref. [32], where a detailed treatment is given): For the dimer model, this is obvious since $\langle D' | D \rangle = \delta_{D, D'}$ and thus $h' = h + \text{const}$, and for the RVB model, configurations where D and D' differ more than locally give rise to longer and thus to fewer loops in the overlap $\langle \sigma_g(D) | \sigma_g(D') \rangle$ [Fig. 1(f)], which are thus suppressed [each loop gives a factor 2 in $\langle \sigma_g(D) | \sigma_g(D') \rangle$]; a more formal argument follows Ref. [32], where $\langle \Psi_g | \Psi_g \rangle$ is mapped to a dimer model with an irrelevant interaction.

Since moreover changing $h(\vec{x}) \rightarrow h(\vec{x}) + 4$ in a region leaves the pattern locally invariant, this leads us to a compactified field (see Refs. [29–31] for a detailed discussion) $\phi(\vec{x}) = \frac{\pi}{2} h(\vec{x}) \in [0; 2\pi)$ governed by an effective $(2+0)D$ field theory, which captures the long-wavelength physics of

the dimer and RVB model [29–31],

$$S_{\text{free},K} = \frac{1}{8\pi K} \int d\vec{x} (\vec{\nabla}\phi)^2, \quad (1)$$

where for the dimer model, $K = 1$ is known analytically.

The RVB PEPS with tensor P can be naturally generalized to include LR singlets, by adding a tensor Q consisting of terms [see Fig. 1(c)] which additionally entangle two of the virtual indices through a singlet (a “teleportation bond”) around corners with suitable weights λ_L and λ_R , and thus give rise to singlets between non-NN sites [26,27]. Specifically, Ref. [27] chooses $\lambda_L = \lambda_R > 0$, while Ref. [26] chooses $-\lambda_L = \lambda_R > 0$; we cover both with a single parameter λ , where $\lambda_L = \lambda$ and $\lambda_R = |\lambda|$, and additionally we define $\tilde{\lambda} = \sqrt{6}\lambda$ (the parameters used in Refs. [26] and [27], respectively).¹ The perturbation $P \rightarrow P + \lambda Q$ breaks the U(1) entanglement symmetry of the tensors down to a \mathbb{Z}_2 symmetry, since the number of virtual 2’s now can be either 1 or 3; on the physical degrees of freedom, this is reflected in the fact that it induces same-sublattice singlets, Fig. 1(e). To mimic this doping in the dimer model, we allow for trivalent objects at vertices [shown in gray in Fig. 1(e)] in addition to dimers, which breaks $U(1) \rightarrow \mathbb{Z}_2$. We call this the dimer-solidomer model; it obeys a \mathbb{Z}_2 Gauss law and can thus be mapped to a \mathbb{Z}_2 loop or vertex model.

For the above PEPS ansatz of doping the RVB model with LR singlets, strong indications for critical behavior up to $0 \leq \tilde{\lambda} \leq 0.85$ and for $\tilde{\lambda} \approx -0.85$ have been observed, as witnessed by an algebraic decay of the correlation functions and extraction of a central charge $c = 1$ from a suitable scaling [26,27]. This suggests that the model for $\lambda \neq 0$ should indeed be described by an effective theory of the form (1), possibly with a different Luttinger parameter K . To further strengthen this point, we extract K in different ways and check for consistency.

On the one hand, we determine K from different two-point correlations. Each operator contains primary fields $e^{i(e\phi+m\theta)}$ with charge e and flux m , with associated scaling dimension

$$[e^{i(e\phi+m\theta)}] \equiv \Delta_{e,m} = Ke^2 + \frac{1}{4K}m^2, \quad (2)$$

where we expect all fields allowed by symmetry considerations to appear. ($[O]$ denotes the scaling dimension of O , and θ is the dual field, $\partial_i\phi = 2K\varepsilon_{ij}\partial_j\theta$.) We use two correlation functions: First, between solitons (i.e., visons, living on plaquettes), which correspond to applying a -1 phase for each dimer along a cut starting at plaquette \vec{x}_0 , or in the PEPS a string of $Z = \text{diag}(-1, -1, 1)$ placed on the bonds, where we compute the overlap with the vacuum; note that this correlator is typically not accessible with other methods. Changing between dimer and no dimer around \vec{x}_0 corresponds to changing $h(\vec{x}_0)$ by ± 4 , and thus the resulting minus sign

¹Note that for $\lambda < 0$, adding the two terms in Fig. 1(c) yields an equivalent representation with only straight teleportation bonds with weight $\lambda_S = \lambda_R = -\lambda_L$, Fig. 1(d). This explains why Ref. [26] did not observe AA-sublattice singlets between diagonally adjacent sites, and it shows that the resulting LR-doped RVB state is very special as it contains LR-singlets solely along the lattice axes.

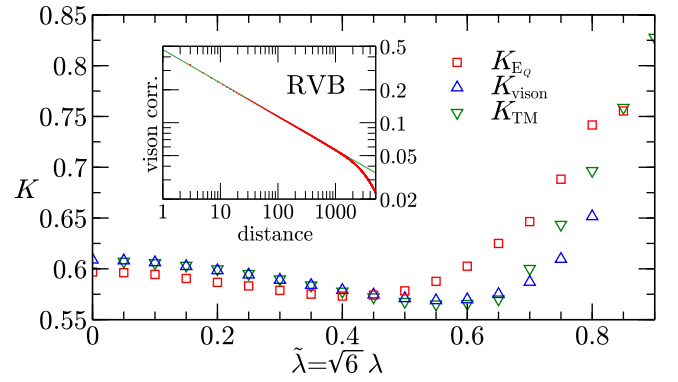


FIG. 2. Luttinger parameter K obtained via different methods: \mathbb{E}_Q and vison correlators ($K_{\mathbb{E}_Q}$, K_{vison}), and finite-size extrapolation ($L = 6, 8$) of the transfer-matrix spectrum (K_{TM}). The good agreement up to $\lambda \approx 0.5$ is consistent with an underlying critical theory. Inset: Decay of vison correlations for the RVB ($\lambda = 0$), obtained with iMPS bond dimension $\chi = 2396$. The correlations show perfect algebraic decay up to a distance of above 1000 sites.

corresponds to an operator $e^{\pm i\phi(\vec{x}_0)/2}$ in the field theory, and thus an electric charge $|e| = \frac{1}{2}$. Second, we consider changing the tensor at a given vertex to one with a reduced \mathbb{Z}_2 symmetry—specifically, a solidomer in the dimer model or a ket-bra pair of Q tensors, which we call \mathbb{E}_Q , for the RVB; since we change $-1 \rightarrow +3$ twice, this corresponds to a magnetic flux $m = \frac{1}{2\pi} \oint \vec{\nabla}\phi \cdot d\vec{r} = \pm 2$, Fig. 1(e). (Since we place the same flux in both ket and bra, the effective field theories of ket and bra vector in the long-wavelength limit can still be described jointly.) The correlation function between a pair of operators with scaling dimension Δ decays as $\ell^{-2\Delta}$ with the separation ℓ , and thus as $\ell^{-K/2}$ and $\ell^{-2/K}$, respectively, for the perturbations considered, which allows us to extract K from numerical boundary iMPS simulations (extrapolating in the finite correlation length induced by the iMPS bond dimension).

In addition, we extract K from the transfer matrix \mathbb{T} , that is, a “slice” of $\langle \Psi_g | \Psi_g \rangle$, on cylinders of circumference L . In the IR, we expect that $\mathbb{T} \sim e^{-H}$, where the field theory of H is the Wick rotated version of (1); for the dimer model, an exact mapping to free fermions and thus a Luttinger liquid with $K = 1$ is indeed known [33,34]. It is well known that the energy spectrum of this (1 + 1)D theory is given by the primaries $E_{e,m} = E_0(L) + \alpha \Delta_{e,m}/L$ for integer e, m and their descendants [35]. For $\frac{1}{2} \leq K \leq 1$, the two dominant subleading eigenvalues of \mathbb{T} correspond to $E_{1,0}$ and $E_{0,1}$, such that we can extract K as $4K^2 = (E_{1,0} - E_{0,0}) / (E_{0,1} - E_{0,0})$.

The results obtained from all three methods are shown in Fig. 2 for the RVB doped with LR singlets; in particular, this also yields an estimate $K = 0.609(10)$ for the nearest-neighbor RVB model, in agreement with earlier estimates from Monte Carlo simulations [31,36]. The good agreement between the results obtained with different methods strengthens the case for a description of the LR-doped model in terms of the effective field theory (1), or equivalently a Luttinger liquid.

The applicability of the effective CFT description (1) suggests that we should be able to use it to assess the stability

of the critical phase under doping with LR singlets, $P \rightarrow P + \lambda Q$. Such perturbations can either be relevant—they open up a gap, and have $\Delta < 2$ —or irrelevant—they disappear under RG, leaving the system critical, and have $\Delta > 2$. If we could show that the perturbation $P + \lambda Q$ which includes LR singlets was irrelevant, this would provide a compelling explanation of the apparent criticality.

To test this hypothesis, we therefore need to determine the scaling dimension of the perturbation $P + \lambda Q$. It is given by the subleading term when expanding $\langle \Psi_g | \Psi_g \rangle = \sum \langle \sigma_g(D) | \sigma_g(D') \rangle$ in orders of λ . The effect of a Q tensor on the A (B) sublattice is to induce a BB (AA) sublattice singlet. Terms $\langle \sigma_g(D) | \sigma_g(D') \rangle$ with a single Q tensor vanish: Each term in the sum is an overlap of singlets, which form closed loops [Fig. 1(f)]; in this overlap, a same-sublattice singlet must always be accompanied by another such singlet. The leading nonzero term is thus second order and consists of pairs of Q tensors. These pairs can appear in two ways: Either an AA and a BB pair in the same (say, ket) layer, or an AA (or BB) pair both in the ket and the bra layer. In both cases, those singlets will be bound together: Otherwise, a long loop appears in the overlap which suppresses it. This can also be understood from symmetry considerations: As we have seen, a single Q tensor on the A (B) sublattice has flux $m = \pm 2$, and since in the long-wavelength limit the magnetic potential ϕ for ket and bra are locked, magnetic fluxes (and thus same-sublattice singlets) must come in pairs with equal ket and bra flux. Moreover, this shows that ket-bra pairs of Q have flux $m = 2$ while ket-ket pairs have flux $m = 0$. In addition, these pairs can also exhibit a nontrivial charge. However, those charges are restricted by lattice symmetries: The smallest nontrivial charge consistent with C_{4v} is $e = 4$ [30], which by itself is an irrelevant perturbation for $K > 1/8$.

It follows that the only potentially relevant perturbation that remains are bound ket-bra pairs of Q operators on the same sublattice. Those have flux $m = 2$ and thus a scaling dimension $\Delta = 1/K$. One might wonder whether there could be cancellation effects (either with pairs nearby, or between Q 's located at different distances), but we have found that summing those correlations converges quickly while not changing our findings, and regrouping does not give rise to cancellations; this is consistent with the fact that such perturbations are allowed by symmetry. We thus find that in second order, doping with LR-singlets can be understood as adding a perturbation with scaling dimension $\Delta = 1/K$. However, for the observed values of $K > \frac{1}{2}$, this implies that $\Delta < 2$ —that is, from a field theory perspective, the perturbation is in fact relevant and *should* open up a gap.

Thus, we find—rather surprisingly—that the effective field theory, which on the one hand seems to describe very well the system at hand, does not explain the existence of an extended critical regime when doping with longer-range singlets, but rather predicts the opening of a gap. So why has it not been observed, and why did our initial tests further support critical behavior? To understand this, let us carry out a scaling analysis. In leading order, the perturbed model is of the form

$$S(\lambda) = \frac{K(\lambda)}{2\pi} \int d^2x (\nabla\theta)^2 + \omega\lambda^2 \int d^2x \cos(2\theta), \quad (3)$$

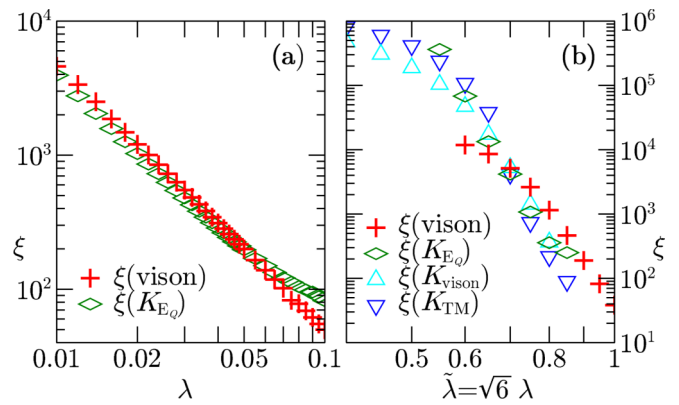


FIG. 3. Correlation length $\xi(\text{vison})$ in the vison sector, and fits $\xi(K)$ obtained from the sine-Gordon model. (a) Dimer-solidomer interpolation. (b) RVB model with LR-singlets, using the K of Fig. 2.

where ω is an as yet unknown parameter that relates the second-order perturbation in Q to $\cos(2\theta)$, and where we have rewritten the free part in terms of the dual field. Note that $K(\lambda)$ has been renormalized due to marginal terms in the perturbation, as we have observed in Fig. 2.

Since $[e^{\pm i2\theta}] = 1/K$, $[\int d^2x \cos(2\theta)] = -2 + 1/K$, and thus for the action to be scale-invariant, $\sqrt{\omega\lambda}$ must scale as $[\sqrt{\omega\lambda}] = 1 - 1/2K$. On the other hand, $[\xi] = -1$, and thus

$$\xi \propto (\sqrt{\omega\lambda})^{-u} \text{ with } u = \left(1 - \frac{1}{2K}\right)^{-1} = \frac{1}{2(K - \frac{1}{2})} + 1. \quad (4)$$

For the dimer model ($K = 1$), we find that $u = 2$, while for the RVB state with $K \approx 0.6$, $u \approx 6$, that is, the correlation length diverges rapidly in the perturbation as long as ω does not change too much, and will thus exceed the previously observed bounds on ξ of a few hundred sites already for moderately large λ . Note that this also implies that on length scales sufficiently below ξ and above the lattice spacing, the system is well described by the free theory. This justifies using the $K(\lambda)$ obtained earlier from fitting the critical correlations at distances sufficiently below ξ , Fig. 2 (i.e., the UV of the sine-Gordon model) to fit $K(\lambda)$ in Eq. (3); cf. Ref. [38].

From this discussion, we conclude that the LR-doped RVB model should be gapped, but with a very large correlation length. To verify these conclusions, we have carried out high-precision simulations using boundary iMPS with bond dimension up to $\chi \approx 2500$ using the SU(2) symmetry and careful state-of-the-art extrapolations [37]. We indeed find finite correlation lengths for all values of $\lambda > 0$ for which we obtain reliable extrapolations, down to $\tilde{\lambda} = 0.6$, where we obtain a correlation length of $\xi \approx 1.2 \times 10^4$, see Fig. 3; below that value, the extrapolation becomes unreliable. To quantitatively compare with the field theory prediction, we first note that Eq. (3) is in fact the sine-Gordon model, for which the gap scaling $\xi = f(K)(\sqrt{\omega\lambda})^{-u}$ with an explicit $f(K)$ is analytically known [38]. To determine ω , we can use that in the UV of the field theory (i.e., below ξ , but above the lattice spacing), the correlations scale as $\langle \cos(2\theta)(\vec{x}) \cos(2\theta)(\vec{y}) \rangle = \frac{1}{2} |x - y|^{-2/K}$ [38]. On the lattice, $\cos(2\theta)$ corresponds to ket-bra pairs of Q tensors; for the dimer-solidomer model,

those have to sit on top of each other, that is, $\mathbb{E}_Q \simeq \omega \cos(2\theta)$, which allows us to determine $\omega \equiv \omega(\lambda)$ from fitting the \mathbb{E}_Q -correlator. This way, we obtain a prediction for ξ without any free parameters [in particular, a potential lattice spacing a drops out, as it then also appears in $\mathbb{E}_Q \simeq a^2 \omega \cos(2\theta)$]. Figure 3(a) shows the prediction for the dimer-solidomer interpolation, which demonstrates a remarkable agreement of the measured data with the field theory prediction, in particular when taking into account that no free parameters were used. For the doped RVB, fitting ω is considerably more difficult, as the ket-bra pairs of Q tensors, which in the IR amount to $\cos(2\theta)$, no longer have to sit on top of each other, even though they remain bound together. As a consequence, it is highly ambiguous how the pairs should be binned in order to give $\omega \cos(2\theta)$ for any given unit volume. An ad-hoc attempt would be to again use the \mathbb{E}_Q -correlator to extract ω , assuming strong binding of the pairs. However, this gives rise to correlations that are about a factor 160 too small, even though they exhibit the correct scaling with $\tilde{\lambda}$, implying that the resulting ω is too large. This suggests that including terms with nearby Q leads to cancellations, which is plausible given the antiferromagnetic nature of the RVB state. Unfortunately, however, there is no unique way in which to group these terms, making a reliable extraction of ω impossible. Furthermore, the uncertainty of ω is amplified in ξ , since $\xi \propto \omega^{-u/2}$, with $u \approx 6$ for the RVB. To still be able to test the CFT prediction, we make the assumption that $\omega \equiv \bar{\omega}$ is independent of $\tilde{\lambda}$. We can then fit this $\bar{\omega}$ by extracting $\omega(\tilde{\lambda})$ from the measured correlation length ξ , and taking $\bar{\omega}$ to be its average over the range $\tilde{\lambda} = 0.6, \dots, 0.8$. The resulting data are shown in Fig. 3(b); in light of the discussed uncertainty in extracting ω , the overly simplistic assumption of a constant $\bar{\omega}$, as well as other error sources (nonrelevant terms might renormalize

interactions, higher orders in λ are no longer negligible), the agreement between the measured ξ and the CFT prediction is still surprisingly good. Similar behavior is observed for $\lambda < 0$, though generally we observe a worse convergence. Let us note that the dominant correlations in the doped RVB are vison correlations (i.e., correlations obtained by placing a Z string in the PEPS), corresponding to the dominant solitons in the sine-Gordon model. The correlations in the spinon sector, on the other hand, are short-ranged even at the U(1) point. In particular, this implies that the doping with long-range singlets induces a gapped topological spin liquid phase with toric code order [39], in accordance with the findings of Ref. [27].

Through this field-theoretic treatment, we thus arrive at the following picture: Perturbing a PEPS with U(1) entanglement symmetry in a way that breaks the symmetry to \mathbb{Z}_2 immediately opens up a gap whenever $K > \frac{1}{2}$ in the effective field theory. However, if K is close to $\frac{1}{2}$ and the perturbation is sufficiently small, the correlation length $\xi \sim \lambda^u$ in the system is extremely large, as $u = 1/2(K - \frac{1}{2}) + 1$. (At $K = \frac{1}{2}$, the system is at a KT point where the correlation length diverges superpolynomially.) Thus, at scales significantly below ξ , but above the lattice spacing (i.e., the UV of the sine-Gordon field theory), the model essentially behaves like a critical Lorentz-invariant theory. At these length scales, PEPS can therefore provide an accurate description of critical systems without enforcing a virtual U(1) symmetry [26,27]. In fact, the best variational PEPS for critical systems can exhibit a rather short correlation length which yet allows for reliable extrapolations [40–42]; it is rather that the very large correlation length we found makes the ansatz hard to converge, which suggests that breaking either lattice or SU(2) symmetries might in fact result in more stable simulations. Note that while guided by the RVB with longer-range singlets, these findings in fact apply to arbitrary PEPS with U(1) entanglement symmetries. In particular, this raises the question of whether SU(2) or SU(N) PEPS ansätze which display chiral features are truly critical (and chiral) away from special U(1)-invariant points [43–47].

Finally, let us return to another one of the original motivations of this work, namely to understand the possibility of emergent symmetries in PEPS. As we have seen, perturbing the U(1) symmetry led to a breakdown of criticality, and thus it is safe to assume that the U(1) symmetry does not reemerge under renormalization. But does this preclude the possibility of emergent U(1) symmetries in 2D PEPS altogether? One way around would be to consider U(1)-breaking perturbations with higher magnetic flux m , while not increasing K ; a possibility for achieving that would be to consider doping of the RVB with N -mers (trimers, tetramers, etc.).

In the following, we present another approach and provide evidence for an emergent U(1) symmetry. As we have observed, the scaling dimension of the \mathbb{Z}_2 perturbation with $m = 2$ is $1/K$, and thus for $K < \frac{1}{2}$ it should become irrelevant. To construct a PEPS with $K < \frac{1}{2}$, we consider the six-vertex model with magnetic field h , where each up-pointing (down-pointing) arrow acquires an additional amplitude $e^{-h/2}$ ($e^{h/2}$); see Fig. 4(a). The fixed point of its transfer matrix is the ground state of the XXZ model with a field, for which $K < \frac{1}{2}$

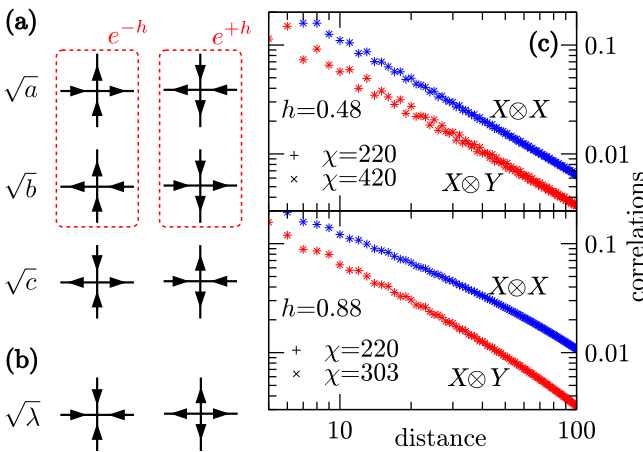


FIG. 4. PEPS with emergent U(1) symmetry. (a) Six-vertex model with magnetic field h ; we choose $a = b = 1, c = 3$. The corresponding PEPS (the superposition of all six-vertex configurations with the indicated amplitude) has $K < \frac{1}{2}$ for suitable h . (b) Perturbation breaking the U(1) symmetry. (c) Decay of correlations related by U(1) but not \mathbb{Z}_2 symmetry. The identical decay scaling at $h = 0.48$ ($K = 0.435$) is consistent with an emergent U(1) symmetry in the correlations, while the different decay at $h = 0.88$ ($K = 0.593$) rules it out. The data converge in the corner transfer matrix (CTM) bond dimension χ .

for suitable parameter choices [48,49] (in particular, there is a finite range of values for h where $K < 1/2$, cf. Fig. A2 of Ref. [49], and thus the same will hold true for the corresponding six-vertex model). The corresponding PEPS is the superposition of all six-vertex configurations with the corresponding weight, obtained by building tensors which carry the arrow configurations both at the physical and the virtual degree of freedom with the corresponding amplitude. We have numerically studied the effect of a perturbation which breaks $U(1)$ to \mathbb{Z}_2 with amplitude $\sqrt{\lambda}$, Fig. 4(b). We choose $h = 0.48$ and 0.88 , where we find $K = 0.435$ and 0.593 , respectively. The field theory predicts that in the former case, we should have an emergent $U(1)$ symmetry at low energies and long distances. To probe this, we measure the correlation functions of two observables that are related by $U(1)$ symmetry at $\lambda = 0$. Specifically, we choose to put Pauli's $X \otimes X$ and $X \otimes Y$ on a ket/bra pair of bonds (the tensor product $A \otimes B$ denotes an operator A on the ket bond and another operator B on the bra bond at a given position); in the field theory, these correspond to $\cos(\theta)$ and $\sin(\theta)$, respectively. These are related by $\theta \rightarrow \theta + \pi/2$, which is no longer a symmetry for $\lambda > 0$. Nevertheless, we find in Fig. 4(c) that their correlation functions decay with the same power law for $K < 1/2$ ($h = 0.48$), as opposed to $K > 1/2$ ($h = 0.88$). In the former case, this leaves the possibility to construct linear combinations of (quasi)local operators which yield $U(1)$ -invariant correlation functions in the IR, while in the latter case this is impossible. Note that the emergent $U(1)$ symmetry does *not* require the two correlators to lie on top of each other: The lattice

operators can generate the field theory operators $\cos \theta$ and $\sin \theta$ with different prefactors, which depend on nonuniversal short-distance properties. This observation is thus consistent with the predicted emergent $U(1)$ symmetry. These results constitute evidence of emergent symmetries in PEPS, which will be investigated further in future work. In particular, it remains to be seen whether such an emergent $U(1)$ symmetry in the correlators can be traced back to emergent virtual $U(1)$ symmetries of the PEPS tensors themselves, such as those recently observed for MPS, e.g., at deconfined quantum critical points [50].

We acknowledge helpful discussions with I. Affleck, P. Fendley, G. Giudici, G. Ortiz, F. Pollmann, and S. Sondhi. H.D., J.Y.C., and N.S. acknowledge support from the European Union's Horizon 2020 program through the ERC-StG WASCOSYS (No. 636201), and from the DFG (German Research Foundation) under Germany's Excellence Strategy (EXC2111-390814868). L.V. is supported by the Research Foundation Flanders. R.V. is supported by the Harvard Quantum Initiative Postdoctoral Fellowship in Science and Engineering, and a grant from the Simons Foundation (No. 376207, Ashvin Vishwanath). The research of N.S. was funded in part by the Austrian Science Fund FWF (Grant DOIs 10.55776/P36305 [51] and 10.55776/F71 [52]) and the European Unions Horizon 2020 research and innovation programme through Grant No. 863476 (ERC-CoG SEQUAM). Computations have been performed in part using the Vienna Scientific Cluster (VSC).

-
- [1] F. Verstraete and J. I. Cirac, Renormalization algorithms for quantum-many body systems in two and higher dimensions, [arXiv:cond-mat/0407066](https://arxiv.org/abs/cond-mat/0407066).
- [2] F. Verstraete, M. M. Wolf, D. Perez-Garcia, and J. I. Cirac, Criticality, the area law, and the computational power of PEPS, *Phys. Rev. Lett.* **96**, 220601 (2006).
- [3] O. Buerschaper, M. Aguado, and G. Vidal, Explicit tensor network representation for the ground states of string-net models, *Phys. Rev. B* **79**, 085119 (2009).
- [4] Z.-C. Gu, M. Levin, B. Swingle, and X.-G. Wen, Tensor-product representations for string-net condensed states, *Phys. Rev. B* **79**, 085118 (2009).
- [5] J. C. Bridgeman and C. T. Chubb, Hand-waving and interpretive dance: An introductory course on tensor networks, *J. Phys. A* **50**, 223001 (2017).
- [6] J. I. Cirac and F. Verstraete, Renormalization and tensor product states in spin chains and lattices, *J. Phys. A* **42**, 504004 (2009).
- [7] U. Schollwöck, The density-matrix renormalization group in the age of matrix product states, *Ann. Phys.* **326**, 96 (2011).
- [8] D. Pérez-García, M. Sanz, C. E. Gonzalez-Guillen, M. M. Wolf, and J. I. Cirac, A canonical form for projected entangled pair states and applications, *New J. Phys.* **12**, 025010 (2010).
- [9] A. Molnar, J. Garre-Rubio, D. Pérez-García, N. Schuch, and J. I. Cirac, Normal projected entangled pair states generating the same state, *New J. Phys.* **20**, 113017 (2018).
- [10] X. Chen, Z. C. Gu, and X. G. Wen, Classification of gapped symmetric phases in one-dimensional spin systems, *Phys. Rev. B* **83**, 035107 (2011).
- [11] N. Schuch, D. Perez-Garcia, and I. Cirac, Classifying quantum phases using matrix product states and projected entangled pair states, *Phys. Rev. B* **84**, 165139 (2011).
- [12] X. Chen, Z.-C. Gu, Z.-X. Liu, and X.-G. Wen, Symmetry protected topological orders and the group cohomology of their symmetry group, *Phys. Rev. B* **87**, 155114 (2013).
- [13] X. Chen, Z.-X. Liu, and X.-G. Wen, 2D symmetry protected topological orders and their protected gapless edge excitations, *Phys. Rev. B* **84**, 235141 (2011).
- [14] S. Jiang and Y. Ran, Symmetric tensor networks and practical simulation algorithms to sharply identify classes of quantum phases distinguishable by short-range physics, *Phys. Rev. B* **92**, 104414 (2015).
- [15] A. Weichselbaum, Non-abelian symmetries in tensor networks: A quantum symmetry space approach, *Ann. Phys.* **327**, 2972 (2012).
- [16] M. Mambrini, R. Orus, and D. Poilblanc, Systematic construction of spin liquids on the square lattice from tensor networks with $SU(2)$ symmetry, *Phys. Rev. B* **94**, 205124 (2016).
- [17] N. Schuch, I. Cirac, and D. Pérez-García, PEPS as ground states: Degeneracy and topology, *Ann. Phys.* **325**, 2153 (2010).
- [18] O. Buerschaper, Twisted injectivity in projected entangled pair states and the classification of quantum phases, *Ann. Phys.* **351**, 447 (2014).

- [19] M. B. Şahinoğlu, D. Williamson, N. Bultinck, M. Marien, J. Haegeman, N. Schuch, and F. Verstraete, Characterizing topological order with matrix product operators, *Ann. Henri Poincaré* **22**, 563 (2021).
- [20] P. W. Anderson, The resonating valence bond state in La_2CuO_4 and superconductivity, *Science* **235**, 1196 (1987).
- [21] R. Moessner and K. S. Raman, Quantum dimer models, in *Introduction to Frustrated Magnetism* (Springer, Berlin, 2010), pp. 437–479.
- [22] X. Chen, B. Zeng, Z. C. Gu, I. L. Chuang, and X. G. Wen, Tensor product representation of topological ordered phase: Necessary symmetry conditions, *Phys. Rev. B* **82**, 165119 (2010).
- [23] L. Balents, Energy density of variational states, *Phys. Rev. B* **90**, 245116 (2014).
- [24] C. Delcamp and N. Schuch, On tensor network representations of the $(3+1)\text{d}$ toric code, *Quantum* **5**, 604 (2021).
- [25] D. J. Williamson, C. Delcamp, F. Verstraete, and N. Schuch, On the stability of topological order in tensor network states, *Phys. Rev. B* **104**, 235151 (2021).
- [26] L. Wang, D. Poilblanc, Z.-C. Gu, X.-G. Wen, and F. Verstraete, Constructing gapless spin liquid state for the spin-1/2 $J_1 - J_2$ Heisenberg model on a square lattice, *Phys. Rev. Lett.* **111**, 037202 (2013).
- [27] J.-Y. Chen and D. Poilblanc, Topological \mathbb{Z}_2 resonating-valence-bond spin liquid on the square lattice, *Phys. Rev. B* **97**, 161107(R) (2018).
- [28] N. Schuch, D. Poilblanc, J. I. Cirac, and D. Pérez-García, Resonating valence bond states in the PEPS formalism, *Phys. Rev. B* **86**, 115108 (2012).
- [29] E. Fradkin, *Field Theories of Condensed Matter Physics* (Cambridge University Press, Cambridge, UK, 2013).
- [30] F. Alet, Y. Ikhlef, J. L. Jacobsen, G. Misguich, and V. Pasquier, Classical dimers with aligning interactions on the square lattice, *Phys. Rev. E* **74**, 041124 (2006).
- [31] Y. Tang, A. W. Sandvik, and C. L. Henley, Properties of resonating-valence-bond spin liquids and critical dimer models, *Phys. Rev. B* **84**, 174427 (2011).
- [32] K. Damle, D. Dhar, and K. Ramola, Resonating valence bond wavefunctions and classical interacting dimer models, *Phys. Rev. Lett.* **108**, 247216 (2012).
- [33] E. H. Lieb, Solution of the dimer problem by the transfer matrix method, *J. Math. Phys.* **8**, 2339 (1967).
- [34] M. Suzuki, The dimer problem and the generalized X-model, *Phys. Lett. A* **34**, 338 (1971).
- [35] P. Di Francesco, P. Mathieu, and D. Sénéchal, *Conformal Field Theory*, Graduate Texts in Contemporary Physics (Springer, New York, 1997).
- [36] A. F. Albuquerque and F. Alet, Critical correlations for short-range valence-bond wave functions on the square lattice, *Phys. Rev. B* **82**, 180408(R) (2010).
- [37] M. M. Rams, P. Czarnik, and L. Cincio, Precise extrapolation of the correlation function asymptotics in uniform tensor network states with application to the Bose-Hubbard and XXZ models, *Phys. Rev. X* **8**, 041033 (2018).
- [38] S. Lukyanov and A. Zamolodchikov, Exact expectation values of local fields in quantum sine-Gordon model, *Nucl. Phys. B* **493**, 571 (1997).
- [39] M. Iqbal and N. Schuch, Entanglement order parameters and critical behavior for topological phase transitions and beyond, *Phys. Rev. X* **11**, 041014 (2021).
- [40] M. Rader and A. M. Lauchli, Finite correlation length scaling in lorentz-invariant gapless iPEPS wave functions, *Phys. Rev. X* **8**, 031030 (2018).
- [41] P. Czarnik and P. Corboz, Finite correlation length scaling with infinite projected entangled pair states at finite temperature, *Phys. Rev. B* **99**, 245107 (2019).
- [42] P. Corboz, P. Czarnik, G. Kapteijns, and L. Tagliacozzo, Finite correlation length scaling with infinite projected entangled-pair states, *Phys. Rev. X* **8**, 031031 (2018).
- [43] D. Poilblanc, J. I. Cirac, and N. Schuch, Chiral topological spin liquids with projected entangled pair states, *Phys. Rev. B* **91**, 224431 (2015).
- [44] D. Poilblanc, N. Schuch, and I. Affleck, $SU(2)_1$ chiral edge modes of a critical spin liquid, *Phys. Rev. B* **93**, 174414 (2016).
- [45] A. Hackenbroich, A. Sterdyniak, and N. Schuch, Interplay of $SU(2)$, point group and translation symmetry for PEPS: Application to a chiral spin liquid, *Phys. Rev. B* **98**, 085151 (2018).
- [46] J.-Y. Chen, L. Vanderstraeten, S. Capponi, and D. Poilblanc, Non-Abelian chiral spin liquid in a quantum antiferromagnet revealed by an iPEPS study, *Phys. Rev. B* **98**, 184409 (2018).
- [47] J.-Y. Chen, S. Capponi, A. Wietek, M. Mambrini, N. Schuch, and D. Poilblanc, $SU(3)_1$ chiral spin liquid on the square lattice: A view from symmetric PEPS, *Phys. Rev. Lett.* **125**, 017201 (2020).
- [48] R. Baxter, *Exactly Solved Models in Statistical Mechanics*, Dover Books on Physics (Dover, Mineola, New York, 2007).
- [49] R. Verresen, A. Vishwanath, and F. Pollmann, Stable Luttinger liquids and emergent $U(1)$ symmetry in constrained quantum chains, [arXiv:1903.09179](https://arxiv.org/abs/1903.09179).
- [50] M. Yang, B. Vanhecke, and N. Schuch, Detecting emergent continuous symmetries at quantum criticality, *Phys. Rev. Lett.* **131**, 036505 (2023).
- [51] <https://doi.org/10.55776/P36305>
- [52] <https://doi.org/10.55776/F71>